ACS OMEGA

http://pubs.acs.org/journal/acsodf Article

# Chemoenzymatic and Protecting-Group-Free Synthesis of 1,4-Substituted 1,2,3-Triazole-α-D-glucosides with Potent Inhibitory Activity toward Lysosomal α-Glucosidase

Jaggaiah N. Gorantla,* Santhi Maniganda, Salila Pengthaisong, Lukana Ngiwsara, Phannee Sawangareetrakul, Suwadee Chokchaisiri, Prasat Kittakoop, Jisnuson Svasti, and James R. Ketudat Cairns*

Cite This: *ACS Omega* 2021, 6, 25710–25719

Read Online

ACCESS | Metrics & More | Article Recommendations | Supporting Information

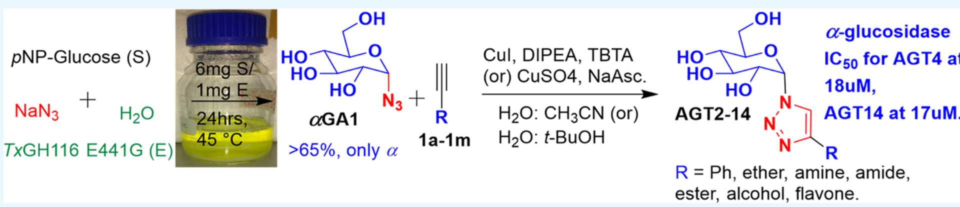


**ABSTRACT:** α-Glucosyl triazoles have rarely been tested as α-glucosidase inhibitors, partly due to inefficient synthesis of their precursor α-D-glucosylazide (**αGA1**). Glycosynthase enzymes, made by nucleophile mutations of retaining β-glucosidases, produce **αGA1** in chemical rescue experiments. *Thermoanaerobacterium xylanolyticus* glucosyl hydrolase 116 β-glucosidase (*Tx*GH116) E441G nucleophile mutant catalyzed synthesis of **αGA1** from sodium azide and *p*NP-β-D-glucoside (*p*NPGlc) or cellobiose in aqueous medium at 45 °C. The *p*NPGlc and azide reaction product was purified by Sephadex LH-20 column chromatography to yield 280 mg of pure **αGA1** (68% yield). **αGA1** was successfully conjugated with alkynes attached to different functional groups, including aryl, ether, amine, amide, ester, alcohol, and flavone via copper-catalyzed azide-alkyne cycloaddition (CuAAC) click chemistry reactions. These reactions afforded the 1,4-substituted 1,2,3-triazole-α-D-glucoside derivatives **AGT2-14** without protection and deprotection. Several of these glucosyl triazoles exhibited strong inhibition of human lysosomal α-glucosidase, with $IC_{50}$ values for **AGT4** and **AGT14** more than 60-fold lower than that of the commercial α-glucosidase inhibitor acarbose.



## ■ INTRODUCTION

Protein engineering has facilitated expansion of the roles of enzymes as green biocatalysts.[1] Biocatalytic methods empower the pharmaceutical sector for the production of large-scale quantities of complex marketed drug intermediates, such as conversion of prositagliptin to stereopure sitagliptin, synthesis of the side chain of atorvastatin, semisynthesis of the antimalarial drug artemisinin and the blockbuster drug paclitaxel, as well as the synthesis of valuable chemicals in ton-scale quantities yearly.[2,3] Thus, biocatalysts are well utilized in various fields.[4−9]

Carbohydrate-active enzymes (CaZymes, www.cazy.org), i.e., glycoside hydrolases, glycosyl transferases, and trans-glycosidases, are described as acting through either a retaining or inverting mechanism, depending on whether the stereochemistry at the bond that is broken is the same or different at the end of the reaction compared to at the beginning.[10] The first (glycosylation) step of the most common retaining mechanism is displacement of a leaving group from the sugar with acid assistance of the catalytic acid/base to protonate the glycosidic bond oxygen and attack by the catalytic nucleophile from the opposite side as the departing bond. In the second (deglycosylation) step, an incoming nucleophile (such as water) is activated by deprotonation by the catalytic acid/base to attack the anomeric carbon of the sugar, displacing the catalytic nucleophile and resulting in a new bond with the same stereochemistry as the initial substrate.

The Withers group and others have demonstrated that retaining glycoside hydrolases in which the catalytic acid/base or nucleophile have been mutated to nonionizable amino acids can be rescued by small nucleophiles and can be used to transglycosylate substrates without hydrolysis of products.[11−14] In fact, the rescue of mutant retaining β-glucosidases using small nucleophiles, such as azide, has become a diagnostic method to identify the catalytic acid/base and catalytic nucleophile.[15−17] The rescue of the catalytic acid/base generally results in a product with the retained anomeric

**Received:** July 23, 2021
**Accepted:** September 10, 2021
**Published:** September 22, 2021

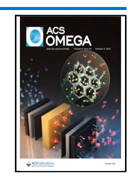

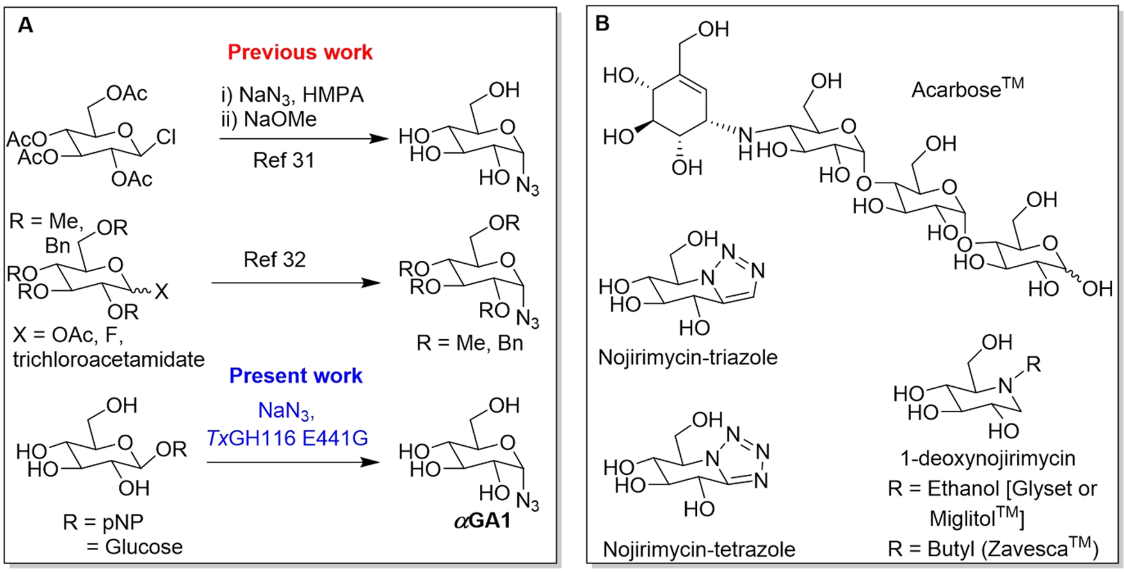


**Figure 1.** (A) Previous and present methods for the synthesis of $\alpha$-D-glucosyl-azide. (B) Structures of reported $\alpha$-glucosidase and glycogen phosphorylase inhibitors.

configuration since the nucleophile is simply taking the place of water in the deglycosylation step. In contrast, the rescue of the nucleophile mutant results in a product with inverted anomeric stereochemistry, since the small nucleophile takes the place of the mutated catalytic nucleophile and the product is released after the glycosylation step. Generally, such products have only been produced in analytical amounts for diagnosis of the role of the mutated residue in the reaction.[17−19]

The catalytic transglycosylation reaction has been well studied and significantly utilized in the production of several useful glycosides, i.e., ester-glycosides,[20] flavonoid-glycosides,[21,22] and $\alpha/\beta$-azido-glycosides.[11,12,15,17,23] Several synthetic routes were reported for the synthesis of 1-azido-$\beta$-D-glucose (also called $\beta$-D-glucosylazide) and well utilized in the area of bioconjugation via click chemistry.[24,25] Numerous copper- and organocatalytic-mediated click reactions were reported in the multidisciplinary chemistry research field.[25−28] Recently, our group reported the gram-scale production of 1-azido-$\beta$-D-glucose via using a retaining $\beta$-glucosidse acid/base-mutant enzyme as the catalyst and utilized it for the synthesis of 1,2,3-triazole-$\beta$-D-glucosides, including a glucosyl Aza-BODIPY dye for enhanced photodynamic cancer therapy applications.[29,30] However, the synthesis and bioactivities of $\alpha$-D-glucosylazide and its triazole glycosides are less well explored, due to the lack of easy synthetic routes. Only a few synthetic methods have been developed for the synthesis of pure $\alpha$-D-glucosylazide (Figure 1A) or its mixture with $\beta$-configured 1-azido-D-glucose via a protection strategy of several steps, and this was subsequently utilized for the synthesis of triazole-$\alpha$-D-glucosides and $\alpha$-D-glucosylamides.[31−34] One set of such triazole-$\alpha$-D-glucosides exhibited weak inhibition against yeast $\alpha$-glucosidase[35] and rabbit muscle glycogen phosphorylase b.[36]

Iminosugars, such as nojirimycin, deoxynojirimycin, and its *N*-alkyl derivatives, have been extensively reported for their $\alpha$-glucosidase inhibitory activities.[37,38] Well-known FDA-approved iminosugar drugs include Miglitol or Glyset and Zavesca, which are used for the treatment of type-II diabetes and the lysosomal storage disorder Gaucher disease, respectively (Figure 1B). 1-Deoxynojirimycin is a strong $\alpha$-glucosidase inhibitor but poor glycogen phosphorylase inhibitor.[39] Nojirimycin-tetrazole and triazole (Figure 1B) bind at the active site through ionic bonding to inhibit glycogen phosphorylase.[40,41] Various nitrogen and other heteroatom-containing glycoconjugates have been reported for their inhibition of $\alpha$-glucosidase activities in yeast,[42] rice,[43] mouse, rat, and human intestine and liver, including lysosomal and endoplasmic reticulum isoenzymes.[44−48]

Iminosugar, azasugar, tetrazole, and triazole glycosides provide strong evidence that the nitrogen-containing glycosides are potential $\alpha$-glucosidase and glycogen phosphorylase (GP) inhibitors. This motivated us to design and assess glucose-conjugated, nitrogen-containing potential $\alpha$-glucosidase inhibitors via short synthetic routes, which might help in treating diabetes and other diseases.

Here, we report the production of $\alpha$-D-glucosylazide **αGA1** (Figure 1A) at the hundreds of milligram scale using the *Thermoanaerobacterium xylanolyticus* glucosyl hydrolase 116 $\beta$-glucosidase (*Tx*GH116) nucleophile mutant *Tx*GH116 E441G as a catalyst. **αGA1** was successfully conjugated with alkynes attached to different functional groups, including aryl, ether, amine, amide, ester, alcohol, uracil, and flavone via copper-catalyzed azide-alkyne cycloaddition (CuAAC) click chemistry reactions. These reactions afforded the 1,4-substituted 1,2,3-triazole-$\alpha$-D-glucoside derivatives **AGT2-14** in good yields by avoiding the protection strategy. Although two of these (**AGT2** and **AGT11**) were previously reported,[35] the remaining ones, **AGT3-10** and **AGT12-14**, have not previously been described, to our knowledge. Among the derivatives, two exhibited 60-fold lower $IC_{50}$ values against human lysosomal $\alpha$-glucosidase compared with the standard inhibitor acarbose (Figure 1B).

## ■ RESULTS AND DISCUSSION

Recently, we showed that *Tx*GH116 E441G was more active in transglycosylation than *Tx*GH116 E441A[17] in the synthesis of $\alpha$-D-glucosylazide and had the most robust catalysis among the *Tx*GH116 nucleophile mutants tested in small-scale rescue and glycosynthase reactions.[49] Therefore, purified *Tx*GH116 E441G enzyme was used for the optimization of the transglucosylation reaction conditions for the formation of


https://doi.org/10.1021/acsomega.1c03928
*ACS Omega* 2021, 6, 25710−25719

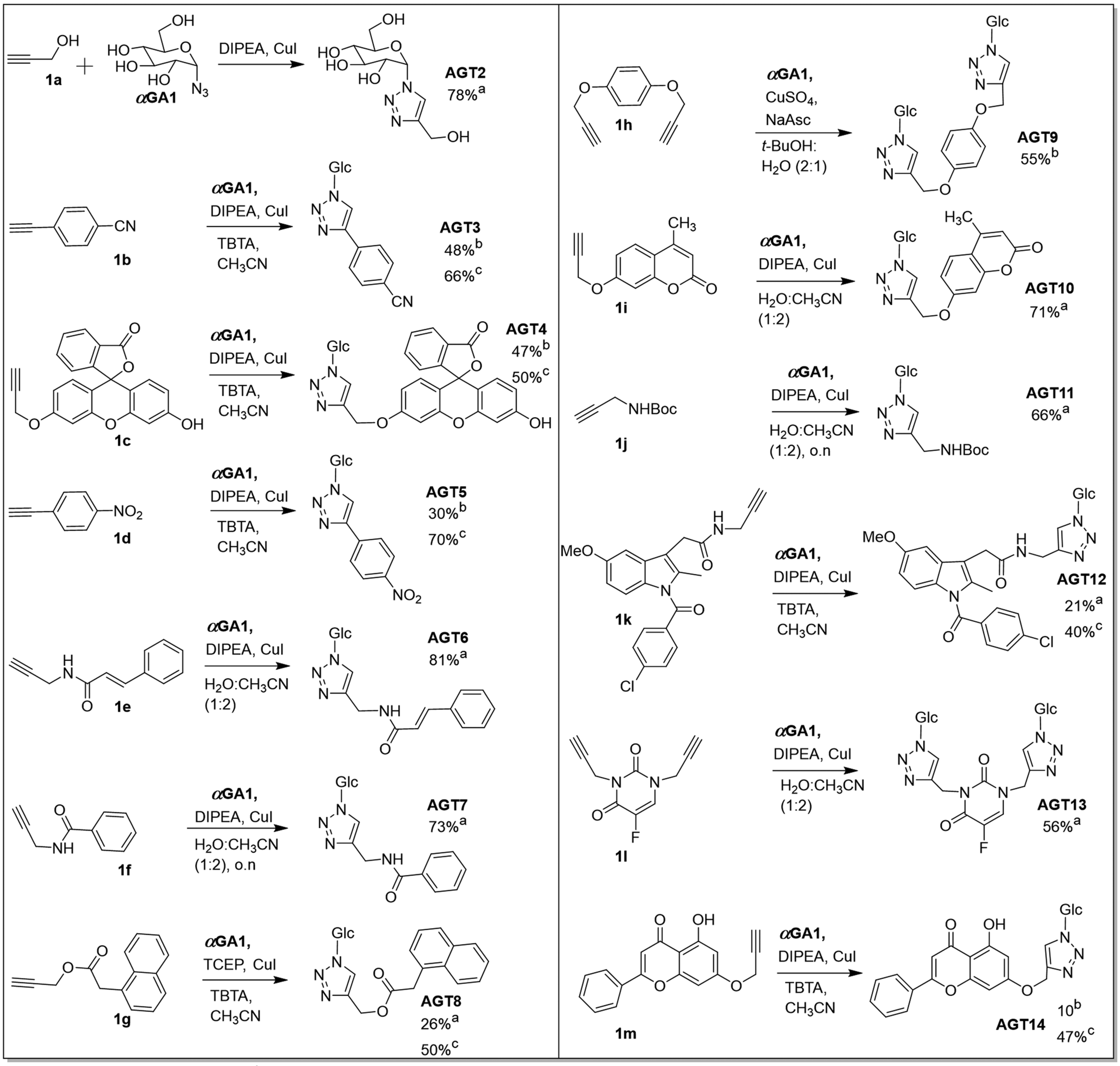


[a]Yields obtained under method A [b]Yields obtained under method B [c]Yields obtained under method C Best yield reaction conditions are shown

**Figure 2.** Synthesis of 1,4-substituted 1,2,3-triazole-$\alpha$-D-glucoside derivatives **AGT2-14** from **αGA1** under click reaction conditions. The amount of 15−30 mg (0.073−0.146 mmol) of **αGA1** was used for each reaction.

**αGA1** in 24 h, by varying the enzyme, *p*-nitrophenyl $\beta$-D-glucopyranoside (*p*NPGlc) and $NaN_3$ concentrations, buffer, pH, and temperature. At the enzyme/substrate ratio, E/S = 1:6, the highest transglucosylation product formation was observed in citrate-phosphate buffer pH 3.5 (final pH 4.6), at 45 or 50 °C, while the concentrations of 100−300 mM $NaN_3$ showed similar results. So, the conditions of 100 mM $NaN_3$ in 100 mM citrate-phosphate buffer, pH 3.5 (pH 4.6 after mixing with azide), and the incubation temperature of 45 °C for 24 h were selected as optimal. With the optimized reaction conditions, the E/S ratio was varied at 1:3, 1:6, and 1:9 (w/w). TLC (Figure S1A) indicated the complete conversion of *p*NPGlc to **αGA1** in E/S (1:3, w/w), and the highest amount of product formation was observed in E/S (1:6, w/w), although some starting material was left unreacted. *Tx*GH116 E441G could also synthesize $\alpha$-D-glucosylazide using cellobiose as the substrate for transglucosylation in the same conditions as used with the *p*NPGlc substrate, but cellobiose gave less $\alpha$-D-glucosylazide product than *p*NPGlc (Figure S1B).

**Scale-Up Synthesis of $\alpha$-D-Glucosylazide (αGA1) Using Enzyme Catalysis.** When the optimized reaction conditions were scaled up to 100 mL with 100 mg of *Tx*GH116 E441G as the catalyst to react 600 mg of *p*NPGlc with 100 mM $NaN_3$, a white solid product was isolated by Sephadex LH-20 chromatography. However, the amount of white solid was more than expected (>1 g) due to the presence of sodium azide that eluted together with $\alpha$-D-glucosylazide. Dissolving the product in methanol and filtering out the undissolved azide afforded 280 mg of **αGA1** in 68% yield as a white solid. **αGA1** was characterized by $^1$H NMR, and the $\alpha$-

anomeric proton chemical shift was observed at $\delta$ 5.51 ppm (H-1, d, $J$ = 4 Hz, 1H). The coupling constant and the spectral values agreed well with those in the literature,[11] as did the C-1 carbon peak, which appeared at $\delta$ 89 ppm in $^{13}$C NMR.

Recently, a similar approach was used to generate a 100 mg quantity of rutinosyl $\alpha$-azide ($\alpha$-L-rhamnopyranosyl (1 → 6) $\alpha$-D-glucopyranosyl azide) in 44% yield from the flavonoid disaccharide rutin with a mutant rutinosidase.[50] This indicates that retaining glycosidase nucleophile mutants have general usefulness for production of synthetically challenging glycosyl azides.

**Synthesis of 1,4-Substituted 1,2,3-Triazole-α-D-glucoside Derivatives (AGT2-14).** Pure **αGA1** was then conjugated with different alkynes attached with variable functional groups, i.e., alcohol, amine, amide, ester, and ether, by the well-known copper-catalyzed azide/alkyne cycloaddition (CuAAC) "click" reactions in $H_2O/CH_3CN$ and $H_2O$/*t*-BuOH, which afforded the set of 1,2,3-triazole-α-D-glucoside derivatives **AGT2-14** (Figure 2). The reaction of propargyl alcohol (**1a**) with **αGA1** and copper(I) iodide (CuI), *N*,*N*-diisopropylethylamine (DIPEA), in $CH_3CN/H_2O$ (2:1) overnight gave **AGT2**[35] in 78% yield as a white solid. The pure alkynes **1e−1g** and **1i−1l** were reacted with **αGA1** in click reactions using the above conditions (Method A) to afford **AGT6**, **AGT7**, **AGT8**, **AGT10**, **AGT11**, **AGT12**, and **AGT13** in 26−81% yields (Figure 2). The ester-conjugated **AGT8** yield was improved from 26 to 50%, by including the additives TBTA and TCEP instead of the base DIPEA. Protected *N*-Boc-propargylamine (**1j**) was synthesized from propargylamine by reacting with $(Boc)_2O$ and triethylamine ($Et_3N$), while **1j** combined with **αGA1** by applying the above conditions (Method A) afforded **AGT11**[35] in 66% yield as a white solid. Our previous experience showing that phenyl acetylenes (**1b**, **1d**) have poor reactivity with unprotected glucosylazide[29] directed us not to follow up the above reaction conditions for these.

Phenyl acetylenes (**1b**, **1d**) were initially dissolved in *t*-BuOH/$H_2O$ (5:1)[36] containing **αGA1** by gentle heating in a water bath, and then, $CuSO_4 \cdot 5H_2O$ and sodium ascorbate were added and stirred for 10 days (method B), which afforded the conjugated products **AGT3** and **AGT5** as white solids in 48 and 30% yields, respectively (Figure 2). **αGA1** reacted with alkyne **1c** in the presence of sodium ascorbate and $CuSO_4 \cdot 5H_2O$, resulting in fluorescein-triazole-glucoside (**AGT4**) in 47% yield (method B). Hydroquinone-dipropargylether (**1h**) was conjugated with azide (**αGA1**) under the above conditions in *t*-BuOH/$H_2O$ (2:1) (method B) and gave a homo-bis-triazole-glucoside ether **AGT9** in 55% yield (Figure 2). The reactions were carried out for longer times to produce the 1,4-addition product in average to good yields. The longer times were required due to the effect of the long bond length of the azide functional group present in **αGA1** compared with the bond length in β-D-glucosylazide.[35,51] We further investigated the different click reaction conditions and improved the yields of **AGT3**, **AGT4**, **AGT5**, and **AGT8** using the additive TBTA along with CuI and DIPEA in acetonitrile (method C).[52] Chrysin-7-propargyl ether (**1m**) was reacted with **αGA1** under the above reaction conditions (method C) to give a chrysin-conjugated triazole **AGT14** in 47% yield (Figure 2).

**Lysosomal α-Glucosidase Inhibition.** The human lysosomal α-glucosidase enzyme has previously been shown to be inhibited by conduritol B epoxide, deoxynojirimycin, and acarbose.[53−55] All of the derivatives were screened for their glucosidase inhibitory activity against human lysosomal α-glucosidase in comparison to acarbose. **AGT4**, **AGT8**, **AGT9**, **AGT10**, **AGT12**, and **AGT14** showed higher inhibition than the 66% α-glucosidase inhibition exhibited by acarbose at 1.43 mM concentration (Table 1), so their $IC_{50}$ values were determined. **AGT8**, **AGT9**, **AGT10**, and **AGT12** exhibited $IC_{50}$ values of 447, 227, 137, and 483 μM, respectively (Table 1). **AGT4** and **AGT14** had $IC_{50}$ values of 18 and 17 μM, respectively, which is 60-fold lower than the standard inhibitor acarbose (Figure 1B ($IC_{50}$ 1.10 mM)). The strong inhibition of α-glucosidase activity by **AGT14** correlates with that of the flavone chrysin itself for which an $IC_{50}$ of 77 μM was previously reported, with its derivatives showing even better activity.[56−59] The presence of the glucosyl-triazole moiety may improve the solubility and inhibition of this flavone.

**Table 1. Relative α-Glucosidase Inhibitory Activities and $IC_{50}$ Values of α-D-Glucosyl-triazole Derivatives**

| entry | compound | α-glucosidase inhibition (%)[a] | $IC_{50}$ (μM)[b] |
|---|---|---|---|
| 1 | acarbose | 66 | 1100 ± 0.10 |
| 2 | αGA1 | 09 | ND |
| 3 | AGT2 | 12 | ND |
| 4 | AGT3 | 46 | ND |
| 5 | AGT4 | 100[c] | 18 ± 0.002 |
| 6 | AGT5 | 57 | ND |
| 7 | AGT6 | 56 | ND |
| 8 | AGT7 | 47 | ND |
| 9 | AGT8 | 72 | 447 ± 0.035 |
| 10 | AGT9 | 87 | 227 ± 0.025 |
| 11 | AGT10 | 80 | 137 ± 0.015 |
| 12 | AGT11 | 52 | ND |
| 13 | AGT12 | 77 | 483 ± 0.021 |
| 14 | AGT13 | 18 | ND |
| 15 | AGT14 | 96 | 17 ± 0.001 |

[a]Percentage inhibition of lysosomal α-glucosidase in comparison to extracts incubated with 1.43 mM acarbose, αGA1, and AGT2−AGT14. [b]$IC_{50}$ values were determined by measuring human lysosomal α-glucosidase activity at different concentrations of the best inhibitors, AGT4, AGT8, AGT9, AGT10, AGT12, and AGT14. [c]The absorbance and fluorescence of AGT4 interfered with activity detection at the initial concentration, but AGT4 did show high inhibition at lower concentrations, which did not interfere with the assay.

In conclusion, enzyme *Tx*GH116 E441G was successfully used for the multi-milligram-scale synthesis of **αGA1** in aqueous medium, thereby avoiding the chemical protection strategy. **αGA1** was further joined with different types of alkynes via a 1,2,3-triazole as a linker by click chemistry. A lack of safe and easy methods for preparation has hindered the azide (**αGA1**) utilization and its applications. The present process might be a useful method for the synthesis of **αGA1** at the industrial level if it can be scaled up effectively. Future improvement of the synthesis of **αGA1** from cellobiose and recovery of residual azide may lead to an ecologically friendly **αGA1** synthesis process. The utility of this convenient method for the production of **αGA1** was demonstrated by its application in the synthesis of some novel 1,4-substituted 1,2,3-triazole-*a*-D-glucoside derivatives (**AGT2-14**) in a short route through protecting-group-free synthesis. We also demonstrated the lysosomal α-glucosidase inhibitory activities of all of the derivatives and found that **AGT4** and **AGT14** exhibited 60-fold lower $IC_{50}$ than acarbose on human


https://doi.org/10.1021/acsomega.1c03928
ACS Omega 2021, 6, 25710−25719

lysosomal α-glucosidase. In the future, the use of these compounds as molecular chaperones for mutant lysosomal α-glucosidase found in Pompe disease and as inhibitors to reduce glycemic effects in diabetes will be explored.

## ■ EXPERIMENTAL SECTION

**General Methods and Materials.** Silica gel 60 $F_{254}$ aluminum TLC plates were used to monitor the reactions with short-wavelength ultraviolet light and by charring the TLC plate after spraying with 10% sulfuric acid in ethanol to visualize the spots. Column chromatography was performed on silica gel 60−200 mesh and Sephadex LH-20 resin. Distilled water was used for the reactions and purification. Lyophilization was used for drying the water samples. $^1$H NMR spectra were recorded at 500 MHz and $^{13}$C NMR spectra were recorded at 125 MHz on a Bruker Avance III 500 MHz instrument with a Cryoprobe Prodigy. Either deuterated water ($D_2O$) or deuterated DMSO ($CD_6SO$) was used as the solvent. Chemical shifts are given in parts per million and coupling constants are in hertz. LC-ToF-MS analysis was performed on a Bruker MicrOTOF-Q ESI-MS or a Thermo Scientific Exactive mass spectrometer with ion mass data given in *m*/*z*.

**Production of α-D-Glucosylazide (αGA1).** *Tx*GH116 E441G was prepared according to the previously described method for wild-type and mutant *Tx*GH116 enzymes.[17] Four-liter cultures were used to prepare 100−200 mg of purified *Tx*GH116 E441G enzyme. The **αGA1** yield was optimized in small-scale (0.1−10 mL) reactions in 100 mM citrate-phosphate at different pH values, 100−300 mM sodium azide, and varying concentrations of *p*NPGlc. The optimized reaction conditions were scaled up to 100 mL with 100 mg of *Tx*GH116 E441G as the catalyst to react 600 mg of *p*NPGlc with 100 mM $NaN_3$ in 100 mM citrate-phosphate buffer, pH 3.5 (final pH 4.6 after addition of azide). The reaction was mixed in a fume hood, and the reaction bottle was tightly sealed to prevent exposure to hydrazoic acid vapor. After 24 h incubation at 45 °C, the pH was adjusted to pH 8 with 2 M $Na_2CO_3$ to minimize hydrazoic acid and the yellow reaction mixture was frozen and lyophilized to dryness. The crude transglucosylation reaction mixture was purified by Sephadex LH-20 column chromatography in 100% water and fractions monitored by TLC. When the product-containing fractions were frozen and lyophilized to dryness (overnight), the amount of white solid was more than expected (>1 g) due to the presence of sodium azide that eluted together with α-D-glucosylazide. The white solid was then dissolved with MeOH (40 mL) and then passed through a celite pad. The filtrate was concentrated under vacuum to afford *a*-D-glucosylazide (αGA1, 280 mg) in 68% yield as a white solid. $R_f$ = 0.25 (silica gel TLC with EtOAc/MeOH 9:1 v/v as the solvent); $^1$H NMR ($D_2O$, 500 MHz): δ 5.51 (H-1, d, *J* = 4 Hz, 1H), 3.86 (dd, *J* = 2, 12 Hz, 1H), 3.81−3.77 (m, 1H), 3.74 (dd, *J* = 5, 12 Hz, 1H), 3.63 (dd, *J* = 4.5, 10 Hz, 1H), 3.58 (appt, *J* = 9 Hz, 1H), and 3.39 (appt, *J* = 9 Hz, 1H); $^{13}$C NMR ($D_2O$, 125 MHz) δ 89.1, 73.7, 72.6, 70.6, 69.1, and 60.4; LC-ToF-MS *m*/*z* $[M + Na]^+$ calcd for $C_6H_{11}N_3$ $NaO_5^+$ 228.0596, found 228.0594.

**Preparation of Alkynes (1b−1m) Using the Reported Reaction Conditions.** The amide and ester functional groups containing alkynes **1e**, **1f**, **1g**, and **1k** (Figure 2) were freshly prepared by coupling the propargylamine or propargyl alcohol with carboxylic acids through the well-known standard EDC/DMAP coupling reaction.[60] Both *O* and *N*-propargyl alkynes **1c, 1h, 1i, 1m,** and **1l** were prepared by alkylating the phenolic hydroxyl group or amide −NH by propargyl bromide using sodium hydride.[61] Phenyl acetylenes **1b** and **1d** (Figure 2) were freshly prepared from their respective aldehydes by reacting with the Ohira−Bestmann reagent via the Seyferth−Gilbert homologation reaction.[62]

**General Procedures Followed for the Synthesis of 1,4-Substituted 1,2,3,-Triazole-*a*-D-glucoside Derivatives (AGT2-14).** *Method A (Applied for Synthesis of **AGT2**, **AGT6**, **AGT7**, **AGT8**, **AGT10**, **AGT11**, **AGT12**, and **AGT13**).* To a solution of *a*-D-glucosylazide (**αGA1**) and alkyne (**1a**, **1e**, **1f**, **1g**, **1i**, **1j**, **1k**, and **1l**) in 1.5 mL of $CH_3CN$/$H_2O$ (2:1) were added CuI (2 equiv) and DIPEA (2 equiv) and the resulting yellow precipitated reaction mixture was stirred at room temperature overnight until the formation of major amounts of products. Reaction mixtures were diluted with methanol (5 mL) and then passed through a celite pad by washing with methanol (20−30 mL) for the removal of copper salt. The filtrate was concentrated and adsorbed on silica gel and then loaded on a silica gel column. The yellow nonpolar impurities and unreacted glucosylazide were eluted in MeOH/EtOAc (3−5/97−95%), and then, the desired 1,2,3,-triazole-*a*-D-glucosides were eluted in MeOH/EtOAc (5−10/95−90%).

*Method B (Applied for Synthesis of **AGT3**, **AGT4**, **AGT5**, **AGT9**, and **AGT14**).* A solution of **αGA1** and alkynes (**1b**, **1c**, **1d**, **1h**, and **1m**) in 1.5−2 mL of *t*-BuOH/$H_2O$ (5:1) was heated in a water bath at 50 °C until the reaction mixture became homogeneous, and then, $CuSO_4 \cdot 5H_2O$ (0.2−0.3 equiv) and sodium ascorbate (0.4−0.6 equiv) were added in that order. Reaction mixtures were stirred at room temperature for more than 1 week until the products were formed. Reaction mixtures were diluted with methanol (5 mL) and then passed through celite pads by washing with methanol (20−30 mL) to remove the copper salt. The filtrate was concentrated and adsorbed on silica gel and then loaded on a silica gel column. Unreacted **αGA1**, **AGT3**, **AGT5**, **AGT5**, **AGT9**, and **AGT14** were eluted with MeOH/EtOAc (5−10/95−90%).

*Method C (Applied for Synthesis of **AGT3**, **AGT4**, **AGT5**, **AGT8**, **AGT12**, and **AGT14**).* This method improved the yields of **AGT3**, **AGT4**, **AGT5**, **ATG8**, **ATG12**, and **ATG14**. To a solution of **αGA1** and alkyne (**1b**, **1c**, **1d**, **1g**, **1k**, or **1m**) dissolved in 1.5 mL of $CH_3CN$ were added CuI (3 equiv), DIPEA (3 equiv), and TBTA (0.5 equiv). TCEP (0.4 equiv) was used instead of DIPEA for the synthesis of **AGT8**. The reaction mixture was stirred at room temperature overnight. Reaction mixtures were diluted with methanol (5 mL) and then passed through a celite pad by washing with methanol (20−30 mL) for the removal of copper salt. The filtrate was concentrated and adsorbed on silica gel and then loaded on a silica column. Unreacted **αGA1**, **AGT3**, **AGT4**, **AGT5**, **ATG8**, and **ATG12** eluted with MeOH/EtOAc (5−10/95−90%), and **AGT14** was purified with MeOH/DCM (5/95%, 8/92%).

*1-(α-D-Glucopyranosyl)-4-hydroxymethyl-[1,2,3]-triazole (**AGT2**).* **αGA1** (20 mg, 0.097 mmol) and propargyl alcohol **1a** (30 μL, 0.485 mmol) reacted following method A to produce **AGT2** as a white solid (20 mg, 78%). The product had silica gel TLC $R_f$ = 0.13 (with EtOAc/MeOH 9:1 v/v as the solvent); $^1$H NMR ($D_2O$, 500 MHz): δ 8.13 (s, 1H), 6.31 (d, *J* = 6 Hz, 1H), 4.75 (s, 2H), 4.43 (appt, *J* = 9 Hz, 1H), 4.13 (dd, *J* = 4, 10 Hz, 1H), 3.77−3.61 (m, 3H), and 3.59 (appt, *J* = 9 Hz, 1H); $^{13}$C NMR ($D_2O$, 125 MHz) δ 146.2, 126.0, 84.9,


https://doi.org/10.1021/acsomega.1c03928
*ACS Omega* 2021, 6, 25710−25719

75.1, 73.1, 70.2, 69.3, 60.2, and 54.4; LC-ToF-MS $m/z$ [M + H]$^+$ calcd for $C_9H_{16}N_3O_6^+$ 262.1039, found 262.1031.

*1-(α-D-Glucopyranosyl)-4-cyano-phenyl-[1,2,3]-triazole (**AGT3**).* **αGA1** (22 mg, 0.107 mmol) and 4-cyano-phenylacetylene **1b** (20 mg, 0.160 mmol) were reacted following method B to produce **AGT3** as a white solid (17 mg, 48%).

**αGA1** (13 mg, 0.063 mmol) and 4-cyano-phenylacetylene **1b** (16 mg, 0.126 mmol) were reacted following method C to produce **AGT3** as a white solid (14 mg, 66%).

**AGT3** had silica gel TLC $R_f$ = 0.19 (with EtOAc/MeOH 9:1 v/v as the solvent); $^1$H NMR (DMSO-$d_6$, 500 MHz): $\delta$ 8.96 (s, 1H), 8.16 (d, $J$ = 8.5 Hz, 2H), 7.94 (d, $J$ = 8.5 Hz, 2H), 6.42 (d, $J$ = 6 Hz, 1H), 5.57 (d, $J$ = 5.0 Hz, 1H), 5.21 (dd, $J$ = 5, 7 Hz, 2H), 4.57 (appt, $J$ = 6 Hz, 1H), 4.21−4.17 (m, 1H), 3.90−3.86 (m, 1H), 3.79−3.76 (m, 1H), 3.71−3.67 (m, 1H), and 3.36−3.34 (m, 1H); $^{13}$C NMR (DMSO-$d_6$, 125 MHz): $\delta$ 144.2, 135.5, 133.5, 126.2, 125.6, 119.3, 110.6, 86.2, 77.2, 73.3, 70.8, 70.3, and 61.2; LC-ToF-MS $m/z$ [M + H]$^+$ calcd for $C_{15}H_{17}N_4O_5^+$ 333.1199, found 333.1206.

*1-(α-D-Glucopyranosyl)-4-methoxy-fluorescein-[1,2,3]-triazole (**AGT4**).* **αGA1** (15 mg, 0.073 mmol) and fluorescein-propargyl ether **1c** (15 mg, 0.0365 mmol) were reacted following method B, and **AGT4** was purified as a yellow solid (10 mg, 47%).

**αGA1** (20 mg, 0.098 mmol) and fluorescein-propargyl ether **1c** (40 mg, 0.098 mmol) were reacted by method C, and **AGT4** was purified as a white solid (28 mg, 50%). The product had silica gel TLC $R_f$ = 0.13 (with EtOAc/MeOH 9:1 v/v as the solvent); $^1$H NMR (DMSO-$d_6$, 500 MHz): $\delta$ 10.23 (s, 1H), 8.44 (s, 1H), 8.07 (d, $J$ = 7.5 Hz, 1H), 7.87 (appt, $J$ = 7.5 Hz, 1H), 7.79 (appt, $J$ = 7.2 Hz, 1H), 7.36 (d, $J$ = 7.5 Hz, 1H), 7.20 (d, $J$ = 2 Hz, 1H), 6.87 (dd, $J$ = 2, 11 Hz, 1H), 6.78 (s, 1H), 6.73 (d, $J$ = 9 Hz, 1H), 6.65 (s, 2H), 6.24 (d, $J$ = 5.5 Hz, 1H), 5.52 (d, $J$ = 5 Hz, 1H), 5.32 (s, 2H), 5.18 (dd, $J$ = 5, 13 Hz, 2H), 4.56 (appt, $J$ = 6 Hz, 1H), 4.17−4.12 (m, 1H), 3.85−3.80 (m, 1H), 3.74 (dd, $J$ = 5, 9.5 Hz, 1H), 3.66 (dd, $J$ = 6, 10.5 Hz, 1H), 3.54−3.50 (m, 1H), and 3.35−3.31 (m, 1H); $^{13}$C NMR (DMSO-$d_6$, 125 MHz): $\delta$ 169.1, 160.2, 160.0, 152.9, 152.3, 152.2, 141.4, 136.1, 130.6, 129.5, 129.4, 127.5, 126.5, 125.1, 124.5, 124.4, 113.3, 112.9, 111.8, 109.9, 102.7, 102.0, 90.2, 85.7, 77.0, 73.4, 70.8, 69.9, 61.8, and 61.1; LC-ToF-MS $m/z$ [M + H]$^+$ calcd for $C_{29}H_{26}N_3O_{10}^+$ 576.1618, found 576.1649.

*1-(α-D-Glucopyranosyl)-4-nitro-phenyl-[1,2,3]-triazole (**AGT5**).* **αGA1** (20 mg, 0.097 mmol) and 4-nitro-phenylacetylene **1d** (36 mg, 0.243 mmol) were reacted following method B, and **AGT5** was purified as a white solid (10 mg, 30%).

To improve the yield, **αGA1** (15 mg, 0.073 mmol) and 4-nitro-phenylacetylene **1d** (21 mg, 0.146 mmol) were reacted following method C and **AGT5** was purified as a white solid (18 mg, 70%).

This compound had silica gel TLC $R_f$ = 0.28 (TLC run twice with EtOAc/MeOH 9:1 v/v as the solvent); $^1$H NMR (DMSO-$d_6$, 500 MHz): $\delta$ 9.09 (s, 1H), 8.41 (d, $J$ = 9 Hz, 2H), 8.25 (d, $J$ = 9 Hz, 2H), 6.28 (d, $J$ = 6 Hz, 1H), 5.60 (d, $J$ = 5 Hz, 1H), 5.22 (dd, $J$ = 5.5, 6.5 Hz, 2H), 4.58 (appt, $J$ = 5.5 Hz, 1H), 4.22−4.17 (m, 1H), 3.91−3.87 (m, 1H), 3.80−3.77 (m, 1H), 3.71−3.68 (m, 1H), 3.57−3.53 (m, 1H) and 3.37−3.35 (m, 1H); $^{13}$C NMR (DMSO-$d_6$, 125 MHz): $\delta$ 147.1, 143.8, 137.4, 126.5, 126.0, 124.8, 86.2, 77.2, 73.3, 70.8, 70.3, and 61.2; LC-ToF-MS $m/z$ [M + H]$^+$ calcd for $C_{14}H_{17}N_4O_7^+$ 353.1097, found 353.1095.

*1-(α-D-Glucopyranosyl)-4-methylene-cinnamide-[1,2,3]-triazole (**AGT6**).* **αGA1** (20 mg, 0.098 mmol) and propargyl-cinnamide **1e** (36 mg, 0.195 mmol) were reacted following method A, and **AGT6** was purified as a white solid (31 mg, 81%). The product had silica gel TLC $R_f$ = 0.15 (with EtOAc/MeOH 9:1 v/v as the solvent); $^1$H NMR ($D_2O$, 500 MHz): $\delta$ 8.12 (s, 1H), 7.63 (appt, $J$ = 3.5 Hz, 2H), 7. 55 (d, $J$ = 15.5 Hz, 1H), 7.46−7.45 (m, 3H), 6.65 (d, $J$ =16 Hz, 1H), 6.30 (d, $J$ = 6 Hz, 1H), 4.62 (s, 2H), 4.44 (appt, $J$ = 9.5 Hz, 1H), 4.14 (dd, $J$ = 5.5, 9.5 Hz, 1H), 3.78−3.72 (m, 3H), and 3.60 (appt, $J$ = 9 Hz, 1H); $^{13}$C NMR ($D_2O$, 125 MHz) $\delta$ 168.8, 141.6, 134.3, 130.3, 129.0, 128.0, 119.8, 85.0, 75.9, 73.1, 70.2, 69.3, 60.3, and 34.5; LC-ToF-MS $m/z$ [M + H]$^+$ calcd for $C_{18}H_{23}N_4O_6^+$ 391.1618, found 391.1628.

*1-(α-D-Glucopyranosyl)-4-methylene-benzamide-[1,2,3]-triazole (**AGT7**).* **αGA1** (20 mg, 0.098 mmol) and propargyl-benzamide **1f** (31 mg, 0.195 mmol) were reacted following method A, and **AGT7** was purified as a white solid (26 mg, 73%). **AGT7** had silica gel TLC $R_f$ = 0.23 (with EtOAc/MeOH 8.5:1.5 v/v as the solvent); $^1$H NMR ($D_2O$, 500 MHz): $\delta$ 8.13 (s, 1H), 7.79 (d, $J$ = 7.5 Hz, 2H), 7.63 (appt, $J$ = 7.0 Hz, 1H), 7.50 (appt, $J$ = 8.0 Hz, 2H), 6.29 (d, $J$ = 6 Hz, 1H), 4.71 (s, 2H), 4.44 (appt, $J$ = 9 Hz, 1H), 4.14 (dd, $J$ = 5.5, 9.5 Hz, 1H), 3.78−3.71 (m, 3H), and 3.60 (appt, $J$ = 9.5 Hz, 1H); $^{13}$C NMR ($D_2O$, 125 MHz): $\delta$ 170.9, 144.2, 133.2, 132.3, 128.8, 127.1, 125.8, 85.0, 75.2, 73.1, 70.3, 69.3, 60.3, and 34.8; LC-ToF-MS $m/z$ [M + H]$^+$ calcd for $C_{16}H_{21}N_4O_6^+$ 365.1461, found 365.1466.

*1-(α-D-Glucopyranosyl)-4-4-napthalene-1acetate-[1,2,3]-triazole (**AGT8**).* **αGA1** (20 mg, 0.097 mmol) and propargyl-1-napthaleneacetate **1g** (43 mg, 0.195 mmol) were reacted following method A, and **AGT8** was purified as a white solid (11 mg, 26%).

To improve the yield, **αGA1** (20 mg, 0.098 mmol) and propargyl-1-napthaleneacetate **1g** (43 mg, 0.195 mmol) were reacted following method C and **AGT8** was isolated as a white solid (21 mg, 50%).

The product had silica gel TLC $R_f$ = 0.2 (TLC run twice with EtOAc/MeOH 9:1 v/v as the solvent); $^1$H NMR (DMSO-$d_6$, 500 MHz): $\delta$ 8.32 (s, 1H), 8.02−7.98 (m, 2H), 7.94 (dd, $J$ = 2, 7.0 Hz, 1H), 7.63−7.58 (m, 2H), 7.55−7.51 (m, 2H), 6.21 (d, $J$ = 5.5 Hz, 1H), 5.51 (d, $J$ = 5.0 Hz, 1H), 5.27 (s, 2H), 5.19 (dd, $J$ = 5, 7.5 Hz, 2H), 4.58 (appt, $J$ = 5.5 Hz, 1H), 4.26 (s, 2H), 4.16−4.12 (m, 1H), 3.85−3.81 (m, 1H), 3.75−3.73 (m, 1H), 3.69−3.66 (m, 1H), 3.56−3.51 (m, 1H), and 3.36−3.32 (m, 1H); $^{13}$C NMR (DMSO-$d_6$, 125 MHz): $\delta$ 171.5, 140.9, 133.8, 132.2, 131.2, 128.9, 128.5, 12.1, 127.6, 126.7, 126.2, 125.9, 124.4, 85.6, 77.0, 73.3, 70.8, 70.3, 61.2, 57.9, and 38.2; LC-ToF-MS $m/z$ [M + H]$^+$ calcd for $C_{21}H_{24}N_3O_7^+$ 430.1614, found 430.1612.

*1-(α-D-Glucopyranosyl)-4-hydroquinone-methyleneether-[1,2,3]-triazole (**AGT9**).* A solution of **αGA1** (30 mg, 0.146 mmol) and dipropargylated-hydroquinone **1h** (13 mg, 0.073 mmol) was reacted following method B, and **AGT9** was purified as a white solid (24 mg, 55%). Silica gel TLC demonstrated an $R_f$ = 0. 17 (with EtOAc/MeOH 6:4 v/v as the solvent); $^1$H NMR ($D_2O$, 500 MHz): $\delta$ 8.21 (s, 2H), 7.02 (s, 4H), 6.30 (d, $J$ = 6 Hz, 2H), 5.25 (s, 4H), 4.42 (appt, $J$ = 9 Hz, 2H), 4.14 (dd, $J$ = 6, 10 Hz, 2H), 3.74−3.73 (m, 4H), and 3.67−3.59 (m, 4H); $^{13}$C NMR ($D_2O$, 125 MHz): 152.2, 142.8, 127.1, 117.1, 85.1, 75.1, 73.1, 70.2, 69.2, 62.0, and 60.2; LC-ToF-MS $m/z$ [M + Na]$^+$ calcd for $C_{24}H_{32}N_6NaO_{12}^+$ 619.1975, found 619.1974.


https://doi.org/10.1021/acsomega.1c03928
ACS Omega 2021, 6, 25710−25719

*1-(α-D-Glucopyranosyl)-4-methylumbellifery-methyleneether-[1,2,3]-triazole (**AGT10**).* **αGA1** (20 mg, 0.098 mmol) and **1i** (41 mg, 0.195 mmol) were reacted following method A, which generated **AGT10** as a white solid (29 mg, 71%).

Silica gel TLC demonstrated an $R_f$ = 0.14 (with EtOAc/MeOH 8:2 v/v as the solvent); $^1$H NMR (DMSO-$d_6$, 500 MHz): δ 8.46 (s, 1H), 7.78 (d, *J* = 9 Hz, 1H), 7.25 (d, *J* = 2.5 Hz, 1H), 7.14 (dd, *J* = 2.5, 9 Hz, 1H), 6.30 (s, 1H), 6.24 (d, *J* = 6 Hz, 1H), 5.54 (d, *J* = 5 Hz, 1H), 5.37 (s, 2H), 5.19 (dd, *J* = 4.5, 9.5 Hz, 2H), 4.57 (appt, *J* = 5.5 Hz, 1H), 4.17−4.12 (m, 1H), 3.85−3.81 (m, 1H), 3.75−3.72 (m, 1H), 3.68−3.65 (m, 1H), 3.54−3.52 (m, 1H), 3.37−3.32 (m, 1H), and 2,48 (s, 3H); $^{13}$C NMR (DMSO-$d_6$, 125 MHz): δ 161.5, 160.6, 155.1, 153.9, 141.2, 127.6, 127.0, 113.8, 113.0, 111.7, 102.0, 85.73, 77.1, 73.3, 70.8, 70.3, 62.0, 61.2, and 18.6; LC-ToF-MS *m*/*z* $[M + Na]^+$ calcd for $C_{19}H_{21}N_3NaO_8^+$ 442.1226, found 442.1224.

*1-(α-D-Glucopyranosyl)-4-N-Boc-methyleneamine-[1,2,3]-triazole (**AGT11**).* **αGA1** (20 mg, 0.097 mmol) and *N*-Boc-propargylamine **1j** (45 mg, 0.292 mmol) were reacted following method A, resulting in **AGT11** as a white solid (23 mg, 66%). The product had the silica gel TLC $R_f$ = 0.25 (with EtOAc/MeOH 8:2 v/v as the solvent); $^1$H NMR ($D_2O$, 500 MHz): δ 8.05 (s, 1H), 6.29 (d, *J* = 6 Hz, 1H), 4.44 (appt, *J* = 8.5 Hz, 1H), 4.37 (s, 2H), 4.34 (dd, *J* = 6, 10 Hz, 1H), 3.78−3.72 (m, 3H), 3.61 (appt, *J* = 9 Hz, 1H), and 1.43 (s, 9H); $^{13}$C NMR ($D_2O$, 125 MHz): δ 158.0, 125.4, 84.9, 75.1, 73.1, 70.2, 69.3, 60.2, and 27.5; LC-ToF-MS *m*/*z* $[M + H]^+$ calcd for $C_{14}H_{25}N_4O_7^+$ 361.1723, found 361.1739.

*1-(α-D-Glucopyranosyl)-4-methylene-indometacinamide-[1,2,3]-triazole (**AGT12**).* **αGA1** (23 mg, 0.112 mmol) and Indomatecine propargylamine **1k** (62 mg, 0.168 mmol) were reacted following method A, resulting in **AGT12** as a pale-yellow solid (14 mg, 21%).

**αGA1** (20 mg, 0.098 mmol) and Indomatecine propargylamine **1k** (77 mg, 0.195 mmol) underwent a reaction following method C, resulting in **AGT12** as a pale-yellow solid (23 mg, 40%). The silica gel TLC had $R_f$ = 0.25 (with EtOAc/MeOH 8:2 v/v as the solvent); $^1$H NMR (DMSO-$d_6$, 500 MHz): δ 8.57 (s, 1H), 8.01 (s, 1H), 7.68 (d, *J* = 8.5 Hz, 2H), 7.63 (d, *J* = 8.0 Hz, 2H), 7.13 (s, 1H), 6.94 (d, *J* = 9.0 Hz, 1H), 6.70 (d, *J* = 9.0 Hz, 1H), 6.10 (d, *J* = 5.5 Hz, 1H), 5.38 (d, *J* = 4.5 Hz, 1H), 5.08 (d, *J* = 4.0 Hz, 1H), 4.47 (appt, *J* = 5.0 Hz, 1H), 4.34 (d, *J* = 4.5 Hz, 1H), 4.06 (d, *J* = 9.0 Hz, 1H), 3.74 (s, 3H), 3.63−3.61 (m, 1H), 3.55 (s, 2H), 3.46−3.44 (m, 1H), 3.28 (s, 2H) and 2.23 (s, 3H); $^{13}$C NMR (DMSO-$d_6$, 125 MHz): δ 169.8, 168.3, 156.1, 143.9, 138.0, 135.7, 134.7, 131.6, 131.39, 130.8, 129.5, 125.6, 114.9, 114.7, 111.8, 102.4, 85.5, 76.9, 73.4, 70.9, 70.3, 61.3, 55.9, 34.7, 31.5 and 13.9; LC-ToF-MS *m*/*z* $[M + H]^+$ calcd for $C_{28}H_{31}ClN_5O_8^+$ 600.1861, found 600.1884.

*Bis[1-(α-D-glucopyranosyl)]-4-(5-fluorouracil)-N,N′-bis-[methylene-[1,2,3]-triazole] (**AGT13**).* **αGA1** (20 mg, 0.097 mmol) and 5-fluorouracil bis-propargyl **1l** (10 mg, 0.049 mmol) were reacted following method A to yield **AGT13** as a pale-yellow solid (17 mg, 56%). **AGT13** had a silica gel TLC $R_f$ = 0.18 (with EtOAc/MeOH 8:2 v/v as the solvent); $^1$H NMR ($D_2O$, 500 MHz): δ 8.38 (s, 1H), 8.29 (s, 1H), 8.24 (d, *J* = 6.0 Hz, 1H), 6.41 (dd, *J* = 5.5, 6.0 Hz, 2H), 5.47 (s, 2H), 5.31 (s, 2H), 4.56−4.52 (m, 2H), 4.20−4.17 (m, 2H), 3.92−3.87 (m, 2H), 3.73−3.66 (m, 2H), and 3.58 (s, 2H); $^{13}$C NMR ($D_2O$, 125 MHz): δ 170.9, 170.4, 159.0, 155.3, 150.5, 135.1, 129.4, 129.1, 85.2, 85.1, 75.3, 73.1, 70.3, 69.4, 60.4, 48.9, 44.3, 39.2, 36.7 and 33.8; LC-ToF-MS *m*/*z* $[M + H]^+$ calcd for $C_{22}H_{30}FN_8O_{12}^+$ 617.1967, found 617.1984.

*1-(α-D-Glucopyranosyl)-4-chrysinyl-methyleneether-[1,2,3]-triazole (**AGT14**).* **αGA1** (20 mg, 0.098 mmol) and chrysin-propargyl ether **1m** (42 mg, 0.146 mmol) were reacted following method A to yield **AGT14** as a yellow solid (5 mg, 10%).

**αGA1** (20 mg, 0.098 mmol) and chrysin-propargyl ether **1m** (57 mg, 0.195 mmol) were reacted following method C to yield **AGT14** as a yellow solid (17 mg, 47%). **AGT14** had a silica gel TLC $R_f$ = 0.25 (TLC run twice with EtOAc/MeOH 9:1 v/v as the solvent); $^1$H NMR (DMSO-$d_6$, 500 MHz): 12.84 (bs, 1H), 8.43 (s, 1H), 8.13 (s, 1H), 8.11 (s, 1H), 7.65−7.60 (m, 4H), 7.07(s, 1H), 7.01 (s, 1H), 6.55 (s, 1H), 6.21 (d, *J* = 7.5 Hz, 1H), 5.55 (bs, 1H), 5.34 (s, 2H), 5.19 (bs, 1H), 4.55 (bs, 1H), 4.10 (appt, *J* = 11.5 Hz, 1H), 3.80−3.76 (m, 1H), 3.71−3.67 (m, 1H), 3.61b (d, *J* = 14.5 Hz, 1H) and 3.49−3.45 (m, 2H); $^{13}$C NMR (DMSO-$d_6$, 125 MHz): δ 182.1, 164.1, 163.6, 161.2, 157.4, 140.6, 132.2, 130.6, 129.2, 127.3, 126.5, 105.5, 105.2, 98.7, 93.5, 85.3, 76.6, 72.8, 70.4, 69.8, 61.7 and 60.8; LC-ToF-MS *m*/*z* $[M + Na]^+$ calcd for $C_{24}H_{23}N_3NaO_9^+$ 520.1332, found 520.1311.

**α-Glucosidase Inhibitory Activity Assay.** The α-glucosidase inhibitory activity assay was based on a standard fluorometric assay as previously described[63] using human lysosomal α-glucosidase-overexpressing preparations from transiently transfected COS-7 cells.[64] Briefly, the inhibitor was premixed with the appropriate amount of α-glucosidase-overexpressing homogenates (10−30 μg of protein) and incubated for 10 min at 37 °C. Except in the cases of **αGA1**, **AGT2**, **AGT9**, and **AGT11**, which were dissolved in water, the reactions contained 3.5% dimethyl sulfoxide from the inhibitor solutions. Subsequently, 4-methyl-umbelliferyl α-D-glucopyranoside (Sigma-Aldrich, St. Louis, MO) (final concentration = 1.26 mM) in 0.1 M citrate-phosphate buffer, pH 4.0, was added in an incubation mixture of 70 μL. The reaction was incubated for 60 min at 37 °C and was terminated by adding 200 μL of 0.5 M sodium carbonate, pH 10.7, with 0.25 g/L Triton X-100. The release of the product 4-methylumbelliferone was measured at 365 nm excitation/450 nm emission. The control samples were prepared without the inhibitor. The percent inhibition of enzyme activity was calculated using the following formula

$$\text{percent inhibition} = 100\% \times \{(\text{control activity}) - (\text{activity with inhibitor}) / (\text{control activity})\}$$

where control activity is the enzyme activity under the same conditions but without the inhibitor.

The $IC_{50}$ value is defined as the concentration of compound inhibiting 50% of α-glucosidase activity under the stated assay conditions.

## ■ ASSOCIATED CONTENT

### Supporting Information

The Supporting Information is available free of charge at https://pubs.acs.org/doi/10.1021/acsomega.1c03928.

Figure S1, TLC profile of compound αGA1 formation; Figures S2−S29, $^1$H and $^{13}$C NMR spectra of **αGA1** and **AGT2-14**; and Figure S30, LC−MS spectra of **AGT9** (PDF)

## ■ AUTHOR INFORMATION


### Corresponding Authors

**Jaggaiah N. Gorantla** − *Center for Biomolecular Structure, Function and Application, School of Chemistry, Institute of Science, Suranaree University of Technology, Nakhon Ratchasima 30000, Thailand*; Email: gjhnaidu@gmail.com

**James R. Ketudat Cairns** − *Center for Biomolecular Structure, Function and Application, School of Chemistry, Institute of Science, Suranaree University of Technology, Nakhon Ratchasima 30000, Thailand; Laboratory of Biochemistry, Chulabhorn Research Institute, Bangkok 10210, Thailand;* orcid.org/0000-0003-3042-1626; Email: cairns@sut.ac.th

### Authors

**Santhi Maniganda** − *Center for Biomolecular Structure, Function and Application, School of Chemistry, Institute of Science, Suranaree University of Technology, Nakhon Ratchasima 30000, Thailand*

**Salila Pengthaisong** − *Center for Biomolecular Structure, Function and Application, School of Chemistry, Institute of Science, Suranaree University of Technology, Nakhon Ratchasima 30000, Thailand*

**Lukana Ngiwsara** − *Laboratory of Biochemistry, Chulabhorn Research Institute, Bangkok 10210, Thailand*

**Phannee Sawangareetrakul** − *Laboratory of Biochemistry, Chulabhorn Research Institute, Bangkok 10210, Thailand*

**Suwadee Chokchaisiri** − *Center for Biomolecular Structure, Function and Application, School of Chemistry, Institute of Science, Suranaree University of Technology, Nakhon Ratchasima 30000, Thailand*

**Prasat Kittakoop** − *Chulabhorn Graduate Institute, Chemical Sciences Program, Chulabhorn Royal Academy, Bangkok 10210, Thailand;* orcid.org/0000-0002-5210-3162

**Jisnuson Svasti** − *Laboratory of Biochemistry, Chulabhorn Research Institute, Bangkok 10210, Thailand*

Complete contact information is available at: https://pubs.acs.org/10.1021/acsomega.1c03928


### Notes

The authors declare no competing financial interest.

## ■ ACKNOWLEDGMENTS

The authors are thankful to Dr. Yanling Hua for assistance with NMR and LC−MS analyses. Financial support from Suranaree University of Technology, Thailand Science Research and Innovation (TSRI), the Synchrotron Light Research Institute, and the Thailand Research Fund (TRF) grant RSA6280073 is gratefully acknowledged.

## ■ REFERENCES


(1) Denard, C. A.; Ren, H.; Zhao, H. Improving and repurposing biocatalysts via directed evolution. *Curr. Opin. Chem. Biol.* **2015**, *25*, 55−64.

(2) Zhang, M. M.; Su, X.; Ang, E. L.; Zhao, H. Recent advances in biocatalyst development in the pharmaceutical industry. *Pharm. Bioprocess.* **2013**, *1*, 179−196.

(3) Schmid, A.; Dordick, J. S.; Hauer, B.; Kiener, A.; Wubbolts, M.; Witholt, B. Industrial biocatalysis today and tomorrow. *Nature* **2001**, *409*, 258−268.

(4) Sheldon, R. A.; Woodley, J. M. Role of biocatalysis in sustainable chemistry. *Chem. Rev.* **2018**, *118*, 801−838.

(5) Wenda, S.; Illner, S.; Mell, A.; Kragl, U. Industrial biotechnology-the future of green chemistry? *Green Chem.* **2011**, *13*, 3007−3047.

(6) Lăcătuş, M. A.; Bencze, L. C.; Tosa, M. I.; Paizs, C.; Irimie, F.-D. Eco-friendly enzymatic production of 2,5-Bis(hydroxymethyl)furan fatty acid diesters, potential biodiesel additives. *ACS Sustainable Chem. Eng.* **2018**, *6*, 11353−11359.

(7) Ménard, R.; Caillol, S.; Allais, F. Chemo-enzymatic synthesis and characterization of renewable thermoplastic and thermoset isocyanate-free poly(hydroxy)urethanes from ferulic acid derivatives. *ACS Sustainable Chem. Eng.* **2017**, *5*, 1446−1456.

(8) Singh, A.; Falabella, J.; LaPorte, T. L.; Goswami, A. Enzymatic process for N-substituted (3S)- and (3R)-3-hydroxypyrrolidin-2-ones. *Org. Process Res. Dev.* **2015**, *19*, 819−830.

(9) Schrittwieser, J. H.; Resch, V. The role of biocatalysis in the asymmetric synthesis of alkaloids. *RSC Adv.* **2013**, *3*, 17602−17632.

(10) Rye, C. S.; Withers, S. G. Glycosidase mechanisms. *Curr. Opin. Chem. Biol.* **2000**, *4*, 573−580.

(11) Wang, Q.; Graham, R. W.; Trimbur, D.; Warren, R. A. J.; Withers, S. G. Changing enzymic reaction mechanisms by mutagenesis: Conversion of a retaining glucosidase to an inverting enzyme. *J. Am. Chem. Soc.* **1994**, *116*, 11594−11595.

(12) Wang, Q.; Trimbur, D.; Graham, R.; Warren, R. A. J.; Withers, S. G. Identification of the acid/base catalyst in *Agrobacterium faecalis* beta-glucosidase by kinetic analysis of mutants. *Biochemistry* **1995**, *34*, 14554−14562.

(13) Mullegger, J.; Jahn, M.; Chen, H.-M.; Warren, R. A. J.; Withers, S. G. Engineering of a thioglycoligase: Randomized mutagenesis of the acid-base residue leads to the identification of improved catalysts. *Protein Eng., Des. Sel.* **2005**, *18*, 33−40.

(14) Hommalai, G.; Withers, S. G.; Chuenchor, W.; Ketudat Cairns, J. R.; Svasti, J. Enzymatic synthesis of cello-oligosaccharides by rice BGlu1 $\beta$-glucosidase glycosynthase mutants. *Glycobiology* **2007**, *17*, 744−753.

(15) Paal, K.; Ito, M.; Withers, S. G. *Paenibacillus* Sp. TS12 glucosylceramidase: Kinetic studies of a novel sub-family of family 3 glycosidases and identification of the catalytic residues. *Biochem. J.* **2004**, *378*, 141−149.

(16) Cobucci-Ponzano, B.; Aurilia, V.; Riccio, G.; Henrissat, B.; Coutinho, P. M.; Strazzulli, A.; Padula, A.; Corsaro, M. M.; Pieretti, G.; Pocsfalvi, G.; Fiume, I.; Cannio, R.; Rossi, M.; Moracci, M. A new archaeal $\beta$-glycosidase from *Sulfolobus solfataricus*: Seeding a novel retaining $\beta$-glycan-specific glycoside hydrolase family along with the human non-lysosomal glucosylceramidase GBA2. *J. Biol. Chem.* **2010**, *285*, 20691−20703.

(17) Charoenwattanasatien, R.; Pengthaisong, S.; Breen, I.; Mutoh, R.; Sansenya, S.; Hua, Y.; Tankrathok, A.; Wu, L.; Songsiririthigul, C.; Tanaka, H.; Williams, S. J.; Davies, G. J.; Kurisu, G.; Ketudat Cairns, J. R. Bacterial $\beta$-glucosidase reveals the structural and functional basis of genetic defects in human glucocerebrosidase 2 (GBA2). *ACS Chem. Biol.* **2016**, *11*, 1891−1900.

(18) Chuenchor, W.; Pengthaisong, S.; Robinson, R. C.; Yuvaniyama, J.; Oonanant, W.; Bevan, D. R.; Esen, A.; Chen, C.-J.; Opassiri, R.; Svasti, J.; Ketudat Cairns, J. R. Structural insights into rice BGlu1 $\beta$-glucosidase oligosaccharide hydrolysis and transglycosylation. *J. Mol. Biol.* **2008**, *377*, 1200−1215.

(19) Ketudat Cairns, J. R.; Pengthaisong, S.; Luang, S.; Sansenya, S.; Tankrathok, A.; Svasti, J. Protein-carbohydrate interactions leading to hydrolysis and transglycosylation in plant glycoside hydrolase family 1 enzymes. *J. Appl. Glycosci.* **2012**, *59*, 51−62.

(20) Komvongsa, J.; Mahong, B.; Phasai, K.; Hua, Y.; Jeon, J.-S.; Ketudat Cairns, J. R. Identification of fatty acid glucose esters as Os9BGlu31 transglucosidase substrates in rice flag leaves. *J. Agric. Food Chem.* **2015**, *63*, 9764−9769.

(21) Matsuba, Y.; Sasaki, N.; Tera, M.; Okamura, M.; Abe, Y.; Okamoto, E.; Nakamura, H.; Funabashi, H.; Takatsu, M.; Saito, M.; Matsuoka, H.; Nagasawa, K.; Ozeki, Y. A novel glucosylation reaction on anthocyanins catalyzed by acyl-glucose-dependent glucosyltransferase in the petals of carnation and delphinium. *Plant Cell* **2010**, *22*, 3374−3389.

(22) Komvongsa, J.; Luang, S.; Marques, J. V.; Phasai, K.; Davin, L. B.; Lewis, N. G.; Ketudat Cairns, J. R. Active site cleft mutants of Os9BGlu31 transglucosidase modify acceptor substrate specificity and allow production of multiple kaempferol glycosides. *Biochim. Biophys. Acta, Gen. Subj.* **2015**, *1850*, 1405−1414.
(23) Wang, Q.; Withers, S. G. Substrate-assisted catalysis in glycosidases. *J. Am. Chem. Soc.* **1995**, *117*, 10137−10138.
(24) Lim, D.; Brimble, M. A.; Kowalczyk, R.; Watson, A. J. A.; Fairbanks, A. J. Protecting-group-free one-pot synthesis of glycoconjugates directly from reducing sugars. *Angew. Chem., Int. Ed.* **2014**, *53*, 11907−11911.
(25) Tiwari, V. K.; Mishra, B. B.; Mishra, K. B.; Mishra, N.; Singh, A. S.; Chen, X. Cu-catalyzed click reaction in carbohydrate chemistry. *Chem. Rev.* **2016**, *116*, 3086−3240.
(26) Ramachary, D. B.; Shashank, A. B.; Karthik, S. An organocatalytic azide−aldehyde [3+2] cycloaddition: High-yielding regioselective synthesis of 1,4-disubstituted 1,2,3-triazoles. *Angew. Chem., Int. Ed.* **2014**, *53*, 10420−10424.
(27) Shashan, A. B.; Karthik, K.; Madhavachary, R.; Ramachary, D. B. An enolate-mediated organocatalytic azide−ketone [3+ 2] cycloaddition reaction: Regioselective high-yielding synthesis of fully decorated 1, 2, 3-triazoles. *Chem. - Eur. J.* **2014**, *20*, 1−6.
(28) Agrahari, A. K.; Bose, P.; Jaiswal, M. K.; Rajkhowa, S.; Singh, A. S.; Hotha, S.; Mishra, N.; Tiwari, V. K. Cu(I)-catalyzed click chemistry in glycoscience and their diverse applications. *Chem. Rev.* **2021**, 7638−7956.
(29) Gorantla, J. N.; Pengthaisong, S.; Choknud, S.; Kaewpuang, T.; Manyum, T.; Promarak, V.; Ketudat Cairns, J. R. Gram scale production of 1-azido-$\beta$-D-glucose via enzyme catalysis for the synthesis of 1,2,3-triazole-glucosides. *RSC Adv.* **2019**, *9*, 6211−6220.
(30) Treekoon, J.; Pewklang, T.; Chansaenpak, K.; Gorantla, J. N.; Pengthaisong, S.; Lai, R.-Y.; Ketudat-Cairns, J. R.; Kamkaew, A. Glucose conjugated aza-BODIPY for enhanced photodynamic cancer therapy. *Org. Biomol. Chem.* **2021**, *19*, 5867−5875.
(31) Ogawa, T.; Nakabayashi, S.; Shibata, S. Synthetic studies on cell surface glycans, Part XVIII. synthetic studies on nephritogenic glycosides, synthesis of N-($\beta$-L-aspartyl)-$\alpha$-D-glucopyranosylamine. *Agric. Biol. Chem.* **1983**, *47*, 281−285.
(32) Györgydeák, Z.; Szilagyi, L.; Paulsen, H. Synthesis, structure, and reactions of glycosyl azides. *J. Carbohydr. Chem.* **1993**, *12*, 139−163.
(33) Bianchi, A.; Bernardi, A. Traceless staudinger ligation of glycosyl azides with triaryl phosphines: Stereoselective synthesis of glycosyl amides. *J. Org. Chem.* **2006**, *71*, 4565−4577.
(34) Lepage, M. L.; Bodlenner, A.; Compain, P. Stereoselective synthesis of $\alpha$-glycosyl azides by TMSOTf-mediated ring opening of 1,6-anhydro sugars. *Eur. J. Org. Chem.* **2013**, *2013*, 1963−1972.
(35) Dedola, S.; Hughes, D. L.; Nepogodiev, S. A.; Rejzek, M.; Field, R. A. Synthesis of $\alpha$- and $\beta$-d-glucopyranosyl triazoles by CuAAC 'click chemistry': Reactant tolerance, reaction rate, product structure and glucosidase inhibitory properties. *Carbohydr. Res.* **2010**, *345*, 1123−1134.
(36) Bokor, E.; Docsa, T.; Gergely, P.; Somsak, L. Synthesis of 1-(D-glucopyranosyl)-1,2,3-triazoles and their evaluation as glycogen phosphorylase inhibitors. *Bioorg. Med. Chem.* **2010**, *18*, 1171−1180.
(37) *From Synthesis Iminosugars to Therapeutic Applications*; Compain, P.; Martin, O. R., Eds.; John Wiley & Sons Ltd., 2007.
(38) Stutz, A. E. *Iminosugars as Glycosidase Inhibitors: Nojirimycin and Beyond*; Wiley-VCH, 1999.
(39) Ariki, M.; Fukui, T. Affinity of glucose analogs for $\alpha$-glucan phosphorylases from rabbit muscle and potato tubers. *J. Biochem.* **1977**, *81*, 1017−1024.
(40) Mitchell, E. P.; Withers, S. G.; Ermert, P.; Vasella, A. T.; Garman, E. F.; Oikonomakos, N. G.; Johnson, L. N. Ternary complex crystal structures of glycogen phosphorylase with the transition state analogue nojirimycin tetrazole and phosphate in the T and R states. *Biochemistry* **1996**, *35*, 7341−7355.
(41) Heightman, T. D.; Vasella, A.; Tsitsanou, K. E.; Zographos, S. E.; Skamnaki, V. T.; Oikonomakos, N. G. Cooperative interactions of the catalytic nucleophile and the catalytic acid in the inhibition of $\beta$-glycosidases. Calculations and their validation by comparative kinetic and structural studies of the inhibition of glycogen phosphorylase b. *Helv. Chim. Acta* **1998**, *81*, 853−864.
(42) Tanaka, K. S. E.; Winters, G. C.; Batchelor, R. J.; Einstein, F. W. B.; Bennet, A. J. A new structural motif for the design of potent glucosidase inhibitors. *J. Am. Chem. Soc.* **2001**, *123*, 998−999.
(43) Pawar, N. J.; Parihar, V. S.; Chavan, S. T.; Joshi, R.; Joshi, P. V.; Sabharwal, S. G.; Puranik, V. G.; Dhavale, D. $\alpha$-Geminal dihydroxymethyl piperidine and pyrrolidine iminosugars: Synthesis, conformational analysis, glycosidase inhibitory activity, and molecular docking studies. *J. Org. Chem.* **2012**, *77*, 7873−7882.
(44) Bian, X.; Fan, X.; Ke, C.; Luan, Y.; Zhao, G.; Zeng, A. Synthesis and $\alpha$-glucosidase inhibitory activity evaluation of N-substituted aminomethyl-$\beta$-D-glucopyranosides. *Bioorg. Med. Chem.* **2013**, *21*, 5442−5450.
(45) Ishikawa, F.; Jinno, K.; Kinouchi, E.; Ninomiya, K.; Marumoto, S.; Xie, W.; Muraoka, O.; Morikawa, T.; Tanabe, G. Diastereoselective synthesis of salacinol-type $\alpha$-glucosidase inhibitors. *J. Org. Chem.* **2018**, *83*, 185−193.
(46) Asano, N.; Nishida, M.; Kato, A.; Kizu, H.; Matsui, K.; Shimada, Y.; Itoh, T.; Baba, M.; Watson, A. A.; Nash, R. J.; de Lilley, P. M.; Watkin, D. J.; Fleet, G. W. J. Homonojirimycin isomers and N-alkylated homonojirimycins: Structural and conformational basis of inhibition of glycosidases. *J. Med. Chem.* **1998**, *41*, 2565−2571.
(47) Warfield, K. L.; Plummer, E. M.; Sayce, A. C.; Alonzi, D. S.; Tang, W.; Tyrrell, B. E.; Hill, M. L.; Caputo, A. T.; Killingbeck, S. S.; Beatty, P. R.; Harris, E.; Iwaki, R.; Kinami, K.; Ide, D.; Kiappes, J. L.; Kato, A.; Buck, M. D.; King, K.; Eddy, W.; Khaliq, M.; Sampath, A.; Treston, A. M.; Dwek, R. A.; Enterlein, S. G.; Miller, J. L.; Zitzmann, N.; Ramstedt, U.; Shresta, S. Inhibition of endoplasmic reticulum glucosidases is required for in vitro and in vivo dengue antiviral activity by the iminosugar UV-4. *Antiviral Res.* **2016**, *129*, 93−98.
(48) Sayce, A. C.; Alonzi, D. S.; Tyrrell, B. E.; Hill, M. L.; Caputo, A. T.; Kiappes, J. L.; Dwek, R. A.; Miller, J. L.; Zitzmann, N.; Killingbeck, S. S.; Beatty, P. R.; Harris, E.; Iwaki, R.; Kinami, K.; Ide, D.; Kato, A. Iminosugars inhibit dengue virus production via inhibition of ER alpha-glucosidases-not glycolipid processing enzymes. *PLoS Neglected Trop. Dis.* **2016**, *10*, No. e0004524.
(49) Pengthaisong, S.; Hua, Y.; Ketudat Cairns, J. R. Structural basis for transglycosylation in glycoside hydrolase family GH116 glycosynthases. *Arch. Biochem. Biophys.* **2021**, *706*, No. 108924.
(50) Kotik, M.; Brodsky, K.; Halada, P.; Javurkova, H.; Pelantova, H.; Konvalinkova, D.; Bojarova, P.; Kren, V. Access to both anomers of rutinosyl azide using wild-type rutinosidase and its catalytic nucleophile mutant. *Catal. Commun.* **2021**, *149*, No. 106193.
(51) Dedola, S.; Nepogodiev, S. A.; Hughes, D. L.; Field, R. A. 2,3,4,6-Tetra-O-acetyl-$\alpha$-D-glucopyranosyl azide. *Acta Crystallogr., Sect. C: Cryst. Struct. Commun.* **2008**, *64*, o445−o446.
(52) Bouché, L.; Reissig, H. Synthesis of di and trivalent carbohydrate mimetics with oxepane substructure by employing copper-catalyzed [3+2] cycloadditions of alkynes with azido-oxepanes. *Eur. J. Org. Chem.* **2014**, *2014*, 3697−3703.
(53) Hermans, M.; Kroos, M.; Van Beeumen, J.; Oostra, B.; Reuser, A. Human lysosomal alpha-glucosidase. Characterization of the catalytic site. *J. Biol. Chem.* **1991**, *266*, 13507−13512.
(54) Hermans, M. M.; Wisselaar, H.; Kroos, M.; Oostra, B.; Reuser, A. Human lysosomal $\alpha$-glucosidase: Functional characterization of the glycosylation sites. *Biochem. J.* **1993**, *289*, 681−686.
(55) Roig-Zamboni, V.; Cobucci-Ponzano, B.; Iacono, R.; Ferrara, M. C.; Germany, S.; Bourne, Y.; Parenti, G.; Moracci, M.; Sulzenbacher, G. Structure of human lysosomal acid $\alpha$-glucosidase-a guide for the treatment of pompe disease. *Nat. Commun.* **2017**, *8*, No. 1111.
(56) Cheng, N.; Yi, W.-B.; Wang, Q.-Q.; Peng, S.-M.; Zou, X.-Q. Synthesis and $\alpha$-glucosidase inhibitory activity of chrysin, diosmetin, apigenin, and luteolin derivatives. *Chin. Chem. Lett.* **2014**, *25*, 1094−1098.


https://doi.org/10.1021/acsomega.1c03928
ACS Omega 2021, 6, 25710−25719

(57) Proença, C.; Freitas, M.; Ribeiro, D.; Oliveira, E. F. T.; Sousa, J. L. C.; Tome, S. M.; Ramos, M. J.; Silva, A. M. S.; Fernandes, P. A.; Fernandes, E. α-Glucosidase inhibition by flavonoids: An in vitro and in silico structure-activity relationship study. *J. Enzyme Inhib. Med. Chem.* **2017**, *32*, 1216−1228.
(58) Şöhretoğlu, D.; Sari, S.; Barut, B.; Ozel, A. Discovery of potent α-glucosidase inhibitor flavonols: Insights into mechanism of action through inhibition kinetics and docking simulations. *Bioorg. Chem.* **2018**, *79*, 257−264.
(59) Li, K.; Yao, F.; Xue, Q.; Fan, H.; Yang, L.; Li, X.; Sun, L.; Liu, Y. Inhibitory effects against α-glucosidase and α-amylase of the flavonoids. Rich extract from scutellaria baicalensis shoots and interpretation of structure-activity relationship of its eight flavonoids by a refined assign-score method. *Chem. Cent. J.* **2018**, *12*, No. 82.
(60) Naveen; Babu, S. A. EDC/DMAP-mediated direct condensation of dicarboxylic acids and diols: A concise synthesis of extra-large polyether macrocyclic lactones and their X-ray structures. *Tetrahedron Lett.* **2016**, *57*, 5801−5807.
(61) Gorantla, J. N.; Faseela, A.; Lankalapalli, R. S. Design and synthesis of a novel glycosphingolipid derived from polyhydroxy 2-pyrrolidinone and phytoceramide appended by a 1,2,3-triazole linker. *Chem. Phys. Lipids* **2016**, *194*, 158−164.
(62) Roth, G. J.; Liepold, B.; Mueller, S. G.; Bestmann, H. J. Further improvements of the synthesis of alkynes from aldehydes. *Synthesis* **2004**, 59−62.
(63) Okumiya, T.; Keulemans, J. L. M.; Kroos, M. A.; Van der Beek, N. M. E.; Boer, M. A.; Takeuchi, H.; Van Diggelen, O. P.; Reuser, A. J. J. A new diagnostic assay for glycogen storage disease type II in mixed leukocytes. *Mol. Genet. Metab.* **2006**, *88*, 22−28.
(64) Ngiwsara, L.; Wattanasirichaigoon, D.; Tim-Aroon, T.; Rojnueangnit, K.; Noojaroen, S.; Khongkraparn, A.; Sawangareetrakul, P.; Ketudat-Cairns, J. R.; Charoenwattanasatien, R.; Champattanachai, V.; Kuptanon, C.; Pangkanon, S.; Svasti, J. Clinical course, mutations, and its functional characteristics of infantile-onset pompe disease in Thailand. *BMC Med. Genet.* **2019**, *20*, No. 156.


https://doi.org/10.1021/acsomega.1c03928
*ACS Omega* 2021, 6, 25710−25719